Saturn's equinoctial auroras

J. D. Nichols,[1] S. V. Badman,[1] E. J. Bunce,[1] J. T. Clarke,[2] S. W. H. Cowley,[1] F. J. Crary,[3] M. K. Dougherty,[4] J.-C. Gérard,[5] D. Grodent,[5] K. C. Hansen,[6] W. S. Kurth,[7] D. G. Mitchell,[8] W. R. Pryor,[9] T. S. Stallard,[1] D. L. Talboys,[1] and S. Wannawichian[2]

Received 23 October 2009; accepted 24 November 2009; published 23 December 2009.

[1] We present the first images of Saturn's conjugate equinoctial auroras, obtained in early 2009 using the Hubble Space Telescope. We show that the radius of the northern auroral oval is ∼1.5° smaller than the southern, indicating that Saturn's polar ionospheric magnetic field, measured for the first time in the ionosphere, is ∼17% larger in the north than the south. Despite this, the total emitted UV power is on average ∼17% larger in the north than the south, suggesting that field-aligned currents (FACs) are responsible for the emission. Finally, we show that individual auroral features can exhibit distinct hemispheric asymmetries. These observations will provide important context for Cassini observations as Saturn moves from southern to northern summer. **Citation:** Nichols, J. D., et al. (2009), Saturn's equinoctial auroras, *Geophys. Res. Lett.*, *36*, L24102, doi:10.1029/2009GL041491.

1. Introduction

[2] Images of planetary aurora obtained with high-sensitivity instruments onboard HST, e.g., the Advanced Camera for Surveys (ACS), have revolutionised our understanding of outer planetary magnetospheres [e.g., *Grodent et al.*, 2003; *Clarke et al.*, 2009; *Nichols et al.*, 2008], although at Saturn these have exclusively focused on the southern aurora since the wintering northern pole has been hidden from view since 1994. In early 2009 Saturn was approaching equinox, such that the sub-Earth latitude was very low at ∼−2.1°, and the viewpoint from Earth was essentially equatorial providing a roughly similar view of both polar regions. Saturn's internal magnetic field is highly axisymmetric [*Dougherty et al.*, 2005] such that the auroral regions do not cone around the spin axis as they do at, e.g., Jupiter, and were thus constantly visible. In addition, the planet's disk fitted entirely in the field of view of the instrument, such that the northern and southern auroras were imaged simultaneously, in contrast to terrestrial and Jovian auroral observations which generally fit only one pole into the field of view. Such conjugate images provide invaluable insight into the global structure and dynamics of planetary magnetospheres [*Frank and Sigwarth*, 2003; *Østgaard et al.*, 2007; *Laundal and Østgaard*, 2009].

2. Analysis

[3] Approximately 600 images of Saturn's aurora were obtained using ACS in February–March 2009. The images were reduced and projected onto planetocentric latitude-longitude grids as described in the auxiliary material, which also contains Animations S1[10]–S3 of the raw and processed images. An example image is presented in Figure 1, which shows both original and projected views of both the northern and southern auroras. The projections are as seen looking down from above the north pole, and are stretched toward the planet's limb due to the obliquity of the view. Figure 1 and Animations S1–S3 show that auroral emission is generally simultaneously present at the north and south poles, with broadly similar morphology and brightness. Specifically, both poles generally display ovals with an equatorial boundary radius of ∼15°–20°, both are generally brightest in the morning sector, and to first order they vary in a similar manner, i.e., when the northern oval brightens, the southern oval also brightens. This confirms that the processes which excite Saturn's auroral emission are to lowest order hemispherically symmetric. However, important asymmetries are also evident, which we now discuss.

[4] A significant feature of Saturn's ionospheric magnetic field as indicated by models derived from spacecraft magnetometer data [*Dougherty et al.*, 2005] is a substantial difference in magnitude between the north and the south due to the significant quadrupole moment of the field, equivalent to a northward displacement of the magnetic dipole by ∼0.037 R_S (where R_S is the equatorial radius of the 1 bar level equal to 60,268 km). The 'Cassini Saturn Orbit Insertion (SOI)' magnetic field model [*Dougherty et al.*, 2005] gives the magnetic field strength at 15° co-latitude (typical of the auroral oval) and 1,100 km above the 1 bar level (the altitude of maximum auroral brightness [*Gérard et al.*, 2009], equal to ∼55,808 km at 15° co-latitude) to be ∼68,360 and ∼56,643 nT for the north and south, respectively. The difference in field strength between the north and south, relative to the north, at 15° co-latitude is thus ∼17%.

[1]Department of Physics and Astronomy, University of Leicester, Leicester, UK.
[2]Center for Space Physics, Boston University, Boston, Massachusetts, USA.
[3]Division of Space Science and Engineering, Southwest Research Institute, San Antonio, Texas, USA.
[4]Blackett Laboratory, Imperial College London, London, UK.
[5]Laboratoire de Physique Atmosphérique et Planétaire, Université de Liège, Liège, Belgium.
[6]Department of Atmospheric, Oceanic and Space Sciences, University of Michigan, Ann Arbor, Michigan, USA.
[7]Department of Physics and Astronomy, University of Iowa, Iowa City, Iowa, USA.
[8]Johns Hopkins University Applied Physics Laboratory, Laurel, Maryland, USA.
[9]Science Department, Central Arizona College, Coolidge, Arizona, USA.

0094-8276/09/2009GL041491

[10]Auxiliary materials are available in the HTML. doi:10.1029/2009GL041491.

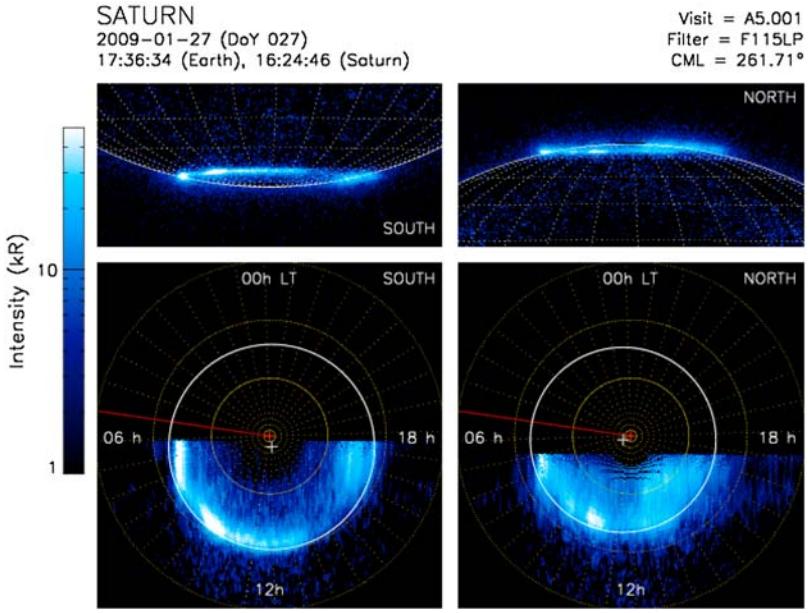

Figure 1. Example image of Saturn's conjugate auroral emission. (left) The southern aurora and (right) the northern aurora are displayed (note that these were originally in the same field of view and are thus simultaneous). (top) The view as observed by HST and (bottom) the planetocentric latitude-longitude projections. The image is shown on a log scale saturated at 50 kR. In each case a 10° × 10° latitude-longitude grid is overlaid. The projections also indicate local times, have the prime meridian highlighted in red, and have the circle fits to the equatorward boundary shown in white. The white crosses show the centre of the fitted circle, whilst the red crosses show the spin pole.

If the auroras occur on a common flux shell in the north and south, as may be expected, they will therefore occur closer to the pole in the north than in the south. The auroral data examined here thus provide an opportunity to test this prediction of the planetary magnetic field models based on magnetometer data necessarily confined to spacecraft trajectories at relatively low latitude and large radial distance.

[5] The location of the equatorial boundary of the auroras in the north and south was determined here using the method used previously to discover the oscillation of the southern auroral oval [*Nichols et al.*, 2008], i.e., by using an algorithm which fits circles to the equatorward boundary of the emission. We used only those images where a sharp equatorward boundary is apparent in both the north and south at all visible longitudes and, owing to the variability of the emission and since the view of each ionosphere is very oblique, this means severely restricting the number of images employed to four. These are shown in auxiliary material, and one is displayed as the example in Figure 1, in which the white circle with the cross at the centre shows the fit. The mean circle radii are ∼16.3° ± 0.6° and ∼17.8° ± 0.4° for the north and south, respectively, the southern value being consistent with previous observations [*Badman et al.*, 2006; *Nichols et al.*, 2008]. The amount of magnetic flux specified by the 'Cassini SOI' model threading the ionosphere poleward of these co-latitudes (a quantity related to the flux function, given for Saturn's internal field by, e.g., *Cowley and Bunce* [2003, equation 1 and Figure 2]) is ∼54.3 ± 3.8 GWb and ∼53.1 ± 2.3 GWb for the north and south, respectively, i.e., essentially the same value of flux within the uncertainty. In addition, the northern radius of 16.3° ± 0.6°, for example, contains ∼45.0 ± 3.2 GWb of flux in the south, i.e., significantly less than the flux contained within the observed radius of the southern oval, confirming the magnetic field model asymmetry.

[6] Bearing in mind these differences in polar magnetic field strength and oval size, we now show in Figure 2 the total observed UV power emitted from the north (Figure 2a) and the south (Figure 2b), obtained by summing the emission over each auroral region. We first note that both hemispheres exhibit emission varying between ∼3 and ∼20 GW, consistent with previous observations of the southern aurora [*Gérard et al.*, 2006; *Clarke et al.*, 2009]. Second, as discussed above, the north and south total emitted powers vary in a broadly similar fashion, such that the linear correlation coefficient between the two is ∼0.81. However, Figure 2c shows the difference between the power emitted from each hemisphere relative to the northern hemisphere. There is a general trend toward greater power observed from the northern hemisphere, with a mean difference of ∼17% of the northern power, a standard deviation of ∼20% and experimental uncertainties of ∼±7% (for details of the experimental method employed to obtain these results, along the uncertainties involved, see the auxiliary material). This difference is particularly striking due to the slightly southern sub-Earth latitude during the observing interval, which results in a greater area of the southern auroral region being visible and which for equal emission would result in the total power observed from the north being reduced to ∼80–90% of the south, i.e., the opposite effect to that observed. Although it is known that the southern auroral oval is generally offset toward midnight by a few degrees [*Nichols et al.*, 2008], simple simulations suggest that in order to produce the observed difference the southern oval would need to be displaced by ∼5° toward midnight while the

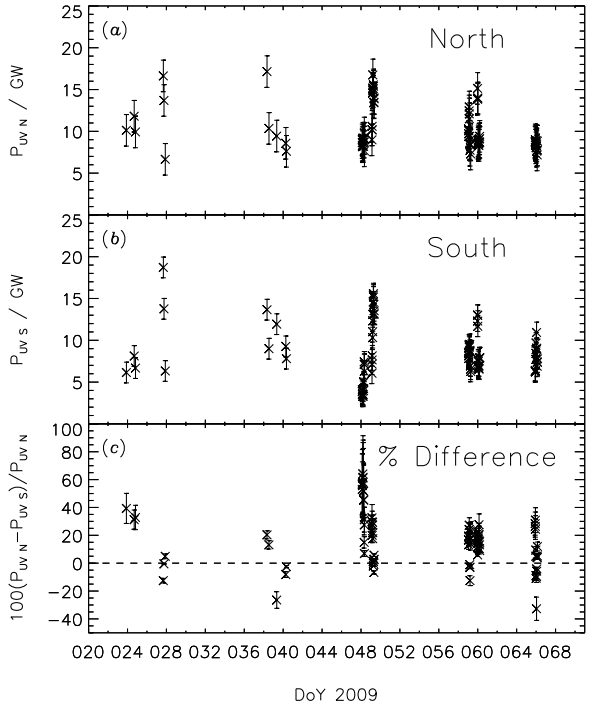

Figure 2. Total UV auroral power emitted from each pole. (a) The power in GW emitted from the north as obtained by summing the entire northern auroral emission in each image obtained using the F115LP filter on the ACS. (b) Similarly shows the power emitted from the southern hemisphere. (c) The difference between the two hemispheres, normalised to the northern power. Errors are calculated as detailed in the auxiliary material.

northern oval remained unshifted, a situation clearly not borne out by the images.

[7] We thus now consider the possible origin of the asymmetry. Liouville's theorem states that for an unaccelerated hot plasma population with a near-isotropic velocity distribution the phase space density function, and thus the particle energy flux, is constant along a given flux tube, such that the total auroral power in this case should be inversely proportional to the ionospheric field strength. This is the opposite effect to that shown by the data here, such that it is likely that the auroras are not produced by this mechanism, rather by field-aligned acceleration of magnetospheric electrons in regions of upward FACs. Theoretical considerations (based on *Knight*'s [1973] kinetic theory and *Cowley et al.*'s [2004] theory of magnetosphere-ionosphere coupling at Saturn, and expounded in the auxiliary material) suggest that the total emitted UV power produced by an axisymmetric layer of upward-directed field-aligned current $I_{\parallel}(= 2\Sigma_P^* \Phi_i \Delta\omega)$ is given by

$$P_{UV} = 0.3 \frac{E_{f\circ}}{j_{\parallel i\circ}{}^2} \frac{\Phi_i{}^2}{\Delta\Phi_i} (\Delta\omega)^2 \Sigma_P^{*2} B_i, \qquad (1)$$

where $j_{\parallel i\circ}$ is the maximum FAC density which can be carried by precipitating magnetospheric plasma alone and $E_{f\circ}$ is the maximum energy flux of the unaccelerated electrons, Φ_i is the magnetic flux threading the ionospheric region enclosed by the auroral annulus, $\Delta\Phi_i$ is the magnetic flux contained within the auroral shell, $\Delta\omega$ is the difference in angular velocity between the plasma at the equatorward and poleward boundaries of the annulus, Σ_P^* is the effective height-integrated Pedersen conductivity, and B_i is the ionospheric magnetic field strength. Assuming the northern and southern auroras lie on the same flux shell, i.e., for fixed Φ_i and $\Delta\Phi_i$, and assuming a common source population, i.e., for fixed $\Delta\omega$, $j_{\parallel i\circ}$, and $E_{f\circ}$, then we have $P_{UV} \propto \Sigma_P^{*2} B_i$. Thus, for identical conductivities, which might be reasonable near equinox, the total field-aligned currents are identical and the total emitted UV power is proportional to the ionospheric field strength. This expectation is consistent with the above result that both the difference in the ionospheric magnetic field strength at 15° co-latitude and the mean difference in the total UV power are ~17%, and we note that [*Cowley et al.*, 2004], who employed more detailed theoretical modeling but also assumed identical conductivities, predicted a similar difference of ~20%. However, we also note that although the conditions were near-equinox, the sub-solar latitude of ~−3.4° was such that at 15° co-latitude the northern and southern solar zenith angles were ~81.1° and ~74.3°, respectively. The ionospheric Pedersen conductivity may have thus been slightly less in the north than in the south, with the expectation on the basis of the above model of decreased northern UV power, although we also note that at Earth additional feedback effects cause the suppression of summer auroras [*Newell et al.*, 1996]. Overall therefore, caveats associated with the Pedersen conductivity aside, these results are consistent with auroral emission produced by similar field-aligned currents, enhanced in the north by increased ionospheric magnetic field strength.

[8] A third significant asymmetry concerns the morphology of individual auroral features. A selection of examples of such asymmetries is shown in Figure 3. We first note that these asymmetric auroral forms are largely responsible for the ~20% standard deviation in the relative difference in total power between the north and south shown in Figure 2c, since the observed power varies as the spots change over time or move over the limb as the planet rotates. Second, bearing in mind the above discussion regarding FACs, we note that these are propagated along the magnetic field as Alfvén waves, and therefore at the local Alfvén speed. The magnetic field threading the southern ionosphere at ~15° co-latitude maps to the equatorial plane at ~15–25 R_S, depending on the size of the magnetosphere [*Bunce et al.*, 2008a], and Cassini field and plasma data suggest that the one-way equator-to-planet Alfvén travel time in this region is around a few hours [*McAndrews et al.*, 2009]. Thus, an Alfvén wave launched from a location, e.g., north of the equatorial plane, would take longer to travel to the southern ionosphere than the northern, possibly leading to asymmetric auroral forms on the time scale of one set of HST images (roughly an hour). Observations of the simultaneous auroras sustained over a few hours would confirm or deny this conjecture. Alternatively, this observation may be related to the recently discovered north-south asymmetry in the Saturn kilometric radiation (SKR) periodicity [*Gurnett et al.*, 2009], and a study of auroral power versus SKR phase

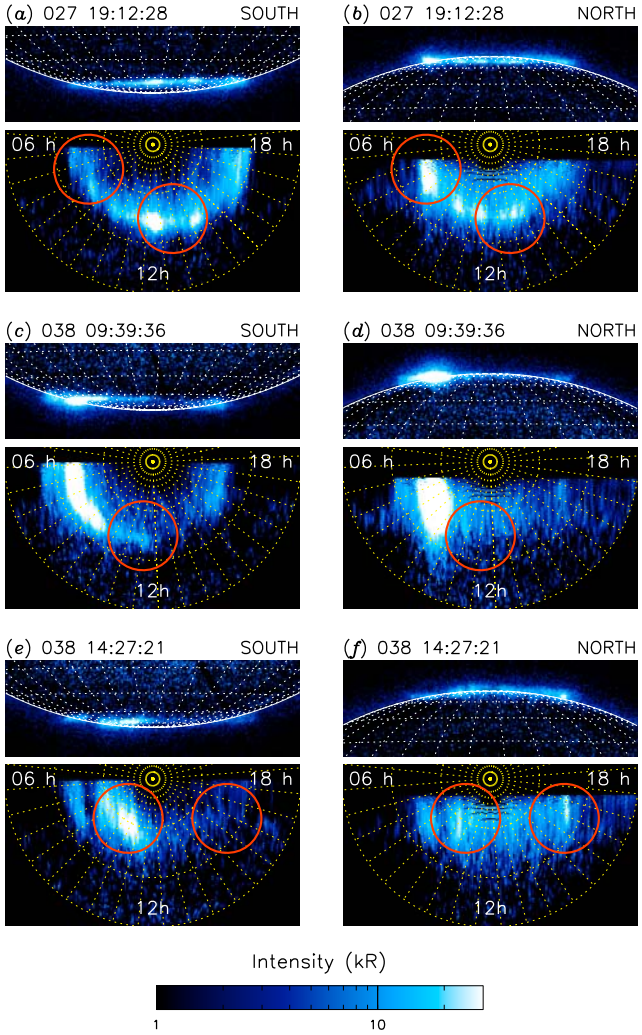

Figure 3. Three examples of images exhibiting hemispherically asymmetric auroral forms. The format of the images is the same as in Figure 1, with (left) the southern aurora and (right) the northern aurora. Obvious asymmetries are highlighted by the red circles.

for both the north and south will determine whether this is the case. On the other hand, small scale variations of the ionospheric Pedersen conductivity, coupled with auroral feedback effects, may lead to localised variations in auroral brightness. It may also be that apparently asymmetric features do have weak corresponding forms in the opposite hemisphere, and a more detailed analysis such as that conducted by *Carbary et al.* [2000] would determine whether this is the case.

3. Summary

[9] We have analysed HST images of Saturn's conjugate equinoctial UV auroras and shown that (a) the radius of the northern auroral oval is $\sim$1.5° smaller than the southern. This result shows that, assuming the north and south auroras lie on the same flux shells (as expected), Saturn's polar magnetic field strengths are consistent with the presence of a significant quadrupole term in the internal field models. (b) The total emitted UV power is on average $\sim$17% larger in the north than the south. This shows that the aurora is not simply produced by precipitating hot magnetospheric plasma, but implies instead the field-aligned acceleration of magnetospheric electrons in regions of upward FACs, as suggested by theoretical models [*Cowley and Bunce*, 2003; *Cowley et al.*, 2004, 2008] and magnetospheric observations [*Bunce et al.*, 2008b; *Talboys et al.*, 2009]. In this case simple theory shows that the total UV power is proportional to the ionospheric magnetic field strength for equal total field-aligned currents in the two ionospheres, as is reasonable at equinox. (c) The two simultaneous ovals can exhibit features that are asymmetric. The cause of these asymmetries is unknown, but possibilities include the short observation timescale relative to the auroral Alfvén wave propagation time, the asymmetric SKR phases, or small scale variations of the Pedersen conductivity.

[10] **Acknowledgments.** This work is based on observations made with the NASA/ESA Hubble Space Telescope, obtained at the Space Telescope Science Institute, which is operated by AURA, Inc. for NASA. JDN, SVB, SWHC, and TSS were supported by STFC grant PP/E000983/1. DLT was supported through STFC grant SG PP/D002117/1. MKD was supported by a STFC grant. Work at Boston was supported by NASA grant HST-GO-10862.01-A from the Space Telescope Science Institute to Boston University. JCG and DG are supported by the Belgian Fund for Scientific Research (FNRS) and the PRODEX Programme managed by the European Space Agency in collaboration with the Belgian Federal Science Policy Office. Research at the University of Iowa is supported by NASA through contract 1356500 with the Jet Propulsion Laboratory. The work at the Johns Hopkins University Applied Physics Laboratory was supported by NASA under contract NAS5-97271.

References

Badman, S. V., S. W. H. Cowley, J.-C. Gérard, and D. Grodent (2006), A statistical analysis of the location and width of Saturn's southern auroras, *Ann. Geophys.*, *24*, 3533–3545.

Bunce, E. J., C. S. Arridge, S. W. H. Cowley, and M. K. Dougherty (2008a), Magnetic field structure of Saturn's dayside magnetosphere and its mapping to the ionosphere: Results from ring current modeling, *J. Geophys. Res.*, *113*, A02207, doi:10.1029/2007JA012538.

Bunce, E. J., et al. (2008b), Origin of Saturn's aurora: Simultaneous observations by Cassini and the Hubble Space Telescope, *J. Geophys. Res.*, *113*, A09209, doi:10.1029/2008JA013257.

Carbary, J. F., K. Liou, A. T. Y. Lui, P. T. Newell, and C. I. Meng (2000), "Blob" analysis of auroral substorm dynamics, *J. Geophys. Res.*, *105*, 16,083–16,091.

Clarke, J. T., et al. (2009), Response of Jupiter's and Saturn's auroral activity to the solar wind, *J. Geophys. Res.*, *114*, A05210, doi:10.1029/2008JA013694.

Cowley, S. W. H., and E. J. Bunce (2003), Corotation-driven magnetosphere-ionosphere coupling currents in Saturn's magnetosphere and their relation to the auroras, *Ann. Geophys.*, *21*, 1691–1707.

Cowley, S. W. H., E. J. Bunce, and J. M. O'Rourke (2004), A simple quantitative model of plasma flows and currents in Saturn's polar ionosphere, *J. Geophys. Res.*, *109*, A05212, doi:10.1029/2003JA010375.

Cowley, S. W. H., et al. (2008), Auroral current systems in Saturn's magnetosphere: Comparison of theoretical models with Cassini and HST observations, *Ann. Geophys.*, *26*, 2613–2630.

Dougherty, M. K., et al. (2005), Cassini magnetometer observations during Saturn orbit insertion, *Science*, *307*, 1266–1270, doi:10.1126/science.1106098.

Frank, L. A., and J. B. Sigwarth (2003), Simultaneous images of the northern and southern auroras from the Polar spacecraft: An auroral substorm, *J. Geophys. Res.*, *108*(A4), 8015, doi:10.1029/2002JA009356.

Gérard, J.-C., B. Bonfond, J. Gustin, D. Grodent, J. T. Clarke, D. Bisikalo, and V. Shematovich (2009), Altitude of Saturn's aurora and its implications for the characteristic energy of precipitated electrons, *Geophys. Res. Lett.*, *36*, L02202, doi:10.1029/2008GL036554.

Gérard, J.-C., et al. (2006), Saturn's auroral morphology and activity during quiet magnetospheric conditions, *J. Geophys. Res.*, *111*, A12210, doi:10.1029/2006JA011965.

Grodent, D., J. T. Clarke, J. Kim, J. H. Waite Jr., and S. W. H. Cowley (2003), Jupiter's main auroral oval observed with HST-STIS, *J. Geophys. Res.*, *108*(A11), 1389, doi:10.1029/2003JA009921.

Gurnett, D. A., A. Lecacheux, W. S. Kurth, A. M. Persoon, J. B. Groene, L. Lamy, P. Zarka, and J. F. Carbary (2009), Discovery of a north-south asymmetry in Saturn's radio rotation period, *Geophys. Res. Lett.*, *36*, L16102, doi:10.1029/2009GL039621.

Knight, S. (1973), Parallel electric fields, *Planet. Space Sci.*, *21*, 741–750, doi:10.1016/0032-0633(73)90093-7.

Laundal, K. M., and N. Østgaard (2009), Asymmetric auroral intensities in the Earth's Northern and Southern hemispheres, *Nature*, *460*, 491–493, doi:10.1038/nature08154.

McAndrews, H. J., et al. (2009), Plasma in Saturn's nightside magnetosphere and the implications for global circulation, *Planet. Space Sci.*, *57*, 1714–1722.

Newell, P. T., C. I. Meng, and K. M. Lyons (1996), Suppression of discrete aurorae by sunlight, *Nature*, *381*, 766–767.

Nichols, J. D., J. T. Clarke, S. W. H. Cowley, J. Duval, A. J. Farmer, J.-C. Gérard, D. Grodent, and S. Wannawichian (2008), Oscillation of Saturn's southern auroral oval, *J. Geophys. Res.*, *113*, A11205, doi:10.1029/2008JA013444.

Østgaard, N., S. B. Mende, H. U. Frey, J. B. Sigwarth, A. Asnes, and J. M. Weygand (2007), Auroral conjugacy studies based on global imaging, *J. Atmos. Sol. Terr. Phys.*, *69*, 249–255, doi:10.1016/j.jastp.2006.05.026.

Talboys, D. L., C. S. Arridge, E. J. Bunce, A. J. Coates, S. W. H. Cowley, and M. K. Dougherty (2009), Characterization of auroral current systems in Saturn's magnetosphere: High-latitude Cassini observations, *J. Geophys. Res.*, *114*, A06220, doi:10.1029/2008JA013846.

S. V. Badman, E. J. Bunce, S. W. H. Cowley, J. D. Nichols, T. S. Stallard, and D. L. Talboys, Department of Physics and Astronomy, University of Leicester, University Road, Leicester LE1 7RH, UK. (jdn@ion.le.ac.uk)

J. T. Clarke and S. Wannawichian, Center for Space Physics, Boston University, 725 Commonwealth Ave., Boston, MA 02215, USA.

F. J. Crary, Division of Space Science and Engineering, Southwest Research Institute, 9503 W. Commerce, San Antonio, TX 78227, USA.

M. K. Dougherty, Blackett Laboratory, Imperial College London, London SW7 2AZ, UK.

J.-C. Gérard and D. Grodent, Laboratoire de Physique Atmosphérique et Planétaire, Université de Liège, Bat. B5c, Allée du 6 Août 17, B-4000 Liège, Belgium.

K. C. Hansen, Department of Atmospheric, Oceanic and Space Sciences, University of Michigan, 2455 Hayward St., Ann Arbor, MI 48109-2143, USA.

W. S. Kurth, Department of Physics and Astronomy, University of Iowa, Iowa City, IA 52241, USA.

D. G. Mitchell, Johns Hopkins University Applied Physics Laboratory, 11100 Johns Hopkins Rd., Laurel, MD 21042, USA.

W. R. Pryor, Science Department, Central Arizona College, 8470 N. Overfield Rd., Coolidge, AZ 85228, USA.